RESEARCH ARTICLE

BORNEO SCIENCE
THE JOURNAL OF SCIENCE & TECHNOLOGY

Journal homepage: https://jurcon.ums.edu.my/ojums/index.php/borneo-science

ADSORPTION BEHAVIOR OF Cu(II), Pb(II), AND Zn(II) ON SELECTED NATURAL SOILS IN SABAH

Tan Wei Hsiang[1], Noumie Surugau[1], Awang Bono[2], Mohd Hardyianto Vai Bahrun[3], Nurika Atiqah Widdie[1], Nur Athirah Suhaimy[1] and Siti Aishah Mohd Ali[1]*

[1] Faculty of Science and Technology, Universiti Malaysia Sabah, Jln UMS, 88400 Kota Kinabalu, Sabah, Malaysia
[2] GRISM Innovative Solutions, 88400 Kota Kinabalu, Sabah, Malaysia
[3] School of Chemical Engineering, Engineering Campus, Universiti Sains Malaysia, 14300 Seri Ampangan, Nibong Tebal, Pulau Pinang, Malaysia

*** Correspondence:**
ctaishah@ums.edu.my

Received: 8 September 2025
Revised: 31 October 2025
Accepted: 2 November 2025
Published online:
3 November 2025

DOI:
10.51200/bsj.v46i2.6789

Keywords:
Adsorption capacity;
Adsorption isotherm models;
Pb^{2+}; Cu^{2+}; Zn^{2+}

ABSTRACT. *Heavy metals in soil can reduce plant fertility and may pose health risks to those who consume the affected plants. Therefore, understanding the soil's ability to retain heavy metals is essential. This study explores the adsorption behaviors of Cu(II), Pb(II), and Zn(II) ions in selected natural soil samples from Sabah, providing insights into their retention capacities and potential environmental implications. The adsorption isotherms were measured using the conventional batch adsorption technique. The results indicate that the adsorption isotherms are satisfactorily described by both the Langmuir and the Freundlich models, with R^2 values mostly exceeding 0.93. Hilltop soil (clay loam) demonstrated the greatest adsorption capacity, exhibiting a distinct metal ion affinity sequence of $Cu^{2+} > Pb^{2+} > Zn^{2+}$. In contrast, clayey sand soils from orchards, rubber plantations, and foothill regions showed a preferential adsorption for Zn^{2+} over Pb^{2+} and Cu^{2+}. Despite sharing similar soil classifications, these variations highlight the influence of site-specific properties on metal ion adsorption behavior. It is found that soil adsorption behavior is shaped by mineralogical composition, particle size distribution, organic matter content, cation exchange capacity, pH, specific surface area, and land management practices. These elements influence both the availability of adsorption sites and the order in which adsorption takes place, ultimately determining the soil's capacity to retain and immobilize substances like heavy metals.*

INTRODUCTION

Soils are the major environmental reservoir for pollutants and waste materials, including heavy metals released through various anthropogenic activities (Naveedullah *et al*., 2013). Due to their nondegradable nature, heavy metals tend to accumulate in soil over time, leading to localized increases in concentration. Uptake of heavy metals from soil to plants is caused by their remaining in food chains, thus becoming a serious issue which may disrupt the balance of the ecosystem (Ayangbenro & Babalola, 2017). The presence of heavy metals also impairs the biodegradation of organic pollutants by disrupting the physiological and ecological functions of microorganisms responsible for organic matter breakdown (Olaniran *et al.*, 2013). Elevated concentrations of heavy metals in soil threaten ecosystem health through direct ingestion, consumption of contaminated water, and bioaccumulation in living organisms.

Furthermore, heavy metal contamination alters soil properties such as pH, porosity, color, and chemical composition, ultimately leading to a decline in overall soil quality (Musilova *et al.,* 2016).

Soil composition plays a pivotal role in regulating its physicochemical properties, particularly pH and cation exchange capacity (CEC), which in turn influence nutrient availability and contaminant mobility. Soil pH can be acidic or basic depending on the parent material during soil formation, while CEC reflects the soil's ability to retain and exchange cations, a function largely attributed to clay minerals and organic matter. Clay particles, with their high surface area and negative charge, exhibit a strong affinity for heavy metal ions such as Pb^{2+}, Cu^{2+}, and Zn^{2+}, facilitating their immobilization through sorption processes (Chen *et al.,* 2023). The presence of organic matter in soil contributes significantly to metal adsorption through complexation and chelation mechanisms (Chenu *et al.,* 2024). Organic compounds possessing functional groups such as carboxyl and phenolic hydroxyls have the capacity to bind metal ions, reducing their mobility and bioavailability. Soil rich in organic content tends to retain heavy metals more effectively, particularly in environments with slightly acidic to neutral pH levels, where these functional groups maintain their reactivity.

Past research has shown that several types of soil were used to adsorb heavy metals (Ali *et al*., 2023; Bai *et al*., 2024). Soil is able to adsorb or retain heavy metals from various sources and accumulates in the soil body. From an environmental perspective, when large quantities of heavy metals are accidentally introduced into the environment, whether through improper waste disposal, accidental spills, or activities like mining and ore smelting, there is concern about whether soils, such as clay-rich soils, can effectively adsorb these metals before they migrate to uncontaminated areas like streams or groundwater. This raises the critical need to assess the adsorption capacity of soils, as their composition significantly influences their ability to retain heavy metals. Soil is a complex matrix composed of various components, each contributing differently to its overall adsorption potential. Even within a single soil component, such as clay minerals, there can be substantial variation in surface area, reactive sites, and mineralogical composition. Clays differ in their chemical structure and arrangement, which affects their interaction with metal ions. Additionally, soil organic matter derived from a wide range of organisms adds another layer of variability, with diverse organic compounds influencing metal binding through various functional groups. Given these complexities, it is important to study the adsorption capacity of soil components in understanding their role in adsorption.

Thus, this study investigates the adsorption behavior of heavy metal ions (Cu^{2+}, Pb^{2+}, and Zn^{2+}) in selected soil samples from Sabah. The batch adsorption technique was used to investigate the adsorption. The adsorption isotherm is described by the most common use models: the Freundlich and Langmuir isotherms.

MATERIALS AND METHODS

Materials and Sampling Sites

Copper (II) ions as copper (II) nitrate trihydrate ($Cu(NO_3)_2.3H_2O$; AR grade, (99%), lead (II) ions as lead (II) nitrate ($Pb(NO_3)_2$; AR grade, (99.0%) and zinc (II) ions as zink (II) nitrate hexahydrate ($Zn(NO_3)_2.6H_2O$; AR grade, (98%). All these reagents were purchased from Sigma-Aldrich. The adsorbents used in this study consist of four soil samples collected from two areas: Kota Marudu and Sepanggar, Sabah. Farm areas (orchard & rubber plantation, Kota Marudu) and areas of different elevations (hilltop & foothill of Botak Hill, Sepanggar) were selected as sites to excavate soil samples. The topsoil layer (about 5 cm) and any discernible plant matter were meticulously removed before the soil samples were obtained from the surface to a depth of 20 cm (ASTM E1727-20). To obtain a representative composite sample, five discrete samples from each station were mixed. All soil samples were dried in an oven for 24 hours at 105 °C and then passed through a sieve (2.0 mm). Table 1 shows the chemical compositions, pH, and organic matter of soil samples.

Table 1. Properties of soil samples.

Soil samples	Chemical composition				pH	Organic matter content (%)
	SiO_2	Al_2O_3	Fe_2O_3	etc		
Orchard	84.20	8.88	4.29	2.62	5.13 ± 0.02	4.38 ± 0.03
Rubber Plantation	85.31	7.81	3.54	3.33	5.22 ± 0.04	1.99 ± 0.01
Hilltop	75.86	15.38	4.86	3.82	4.82 ± 0.09	5.92 ± 0.02
Foothill	81.51	9.35	7.76	1.38	4.41 ± 0.01	4.68 ± 0.03

Particle Size Distribution Analysis

Particle size distribution of sample was determined using the hydrometer method according to ASTM D7928-21E1. The dried samples were subsequently separated based on particle size using a Ro-Tap RX-29 Sieve Shaker. The samples were then transferred to the 2 mm sieve in the Sieve Shaker. With the size of sieves set from the range of 2 mm to 63 µm, the soil samples were separated into their specific size ranges. The percentage of clay, sand, and silt in the soil sample was calculated using Equation 1.

$$\text{Percentage clay/ sand/ silt} = \frac{Mass\ of\ clay,silt\ or\ sand\ in\ soil\ sample\ (g)}{mass\ of\ soil\ sample\ (g)} \times 100\% \quad (1)$$

Surface Area Analysis

Surface area and pore size of the sample were determined using the total surface area (S_t) equation (Equation 2) and the BET equation (Equation 3) (ISO 9277:2010(E)). The samples were degassed at 200 ºC for 1 hour to remove the moisture. Soil samples were analyzed at 79 distinct points to obtain detailed information on pore size distribution and surface area.

$$S_t = N_m A_{CS} \quad (2)$$

Where N_m is the product of the number of molecules of adsorbate in a monolayer and A_{CS} is the effective cross–sectional area of the adsorbate molecule.

$$\frac{1}{W((P/P_o)-1)} = \frac{1}{W_m C} + \frac{C-1}{W_m C}\left(\frac{P}{P_o}\right) \quad (3)$$

Where W is the weight of gas adsorbed (g) at a relative pressure, P/P_o, and W_m is the weight of adsorbate (g) in a monolayer of surface coverage. The term C is the BET constant that is related to the energy of adsorption in the first adsorbed layer, and consequently, its value is an indication of the magnitude of the adsorbent/adsorbate interactions.

Cation Exchangeable Capacity (CEC) Analysis

Cation exchangeable capacity of soil samples was determined by following the SW-846 Test Method 9080. About 3.0 g of the sample was added to a 500 mL Erlenmeyer flask. Then 25 mL of the 1 M ammonium acetate (NH_4OAc) was added and shaken thoroughly, and allowed to stand overnight. The sample was filtered using No.2 filter paper and gently washed four times with 25 mL additions of the NH_4OAc. The leachate was discarded, and the sample was then washed with eight separate additions of 95% ethanol to remove excess saturating solution. Again, the leachate was discarded, and the receiving flask was cleaned. The adsorbed NH_4 was extracted by leaching the sample with eight separate 25 mL additions of 1M potassium chloride (KCl). The leachate was transferred to a 250 mL volumetric flask and diluted to volume with additional KCl. The concentration of NH_4-N in the KCl extract (20 mL) was determined by the Kjeldahl Method (distillation and titration). NH_4-N levels in the original KCl extracting solution (blank) were also measured to account for potential contamination present in the reagent. The CEC value was calculated using Equation 4.

$$\text{CEC (cmol}_c\text{/kg)} = V_a \times N \times V_{KCl} / S \times 100\text{g}/M_s \quad (4)$$

Where V_a is the volume of 0.01N HCl solution (mL) used in titrating the sample, N is the normality of 0.01N HCl solution, S is the volume of filtrate used for distillation (mL), V_{KCl} is the total volume of KCl used to substitute NH_4^+ (mL), and M_s is the weight of the sample used (g).

Adsorption Study

The adsorption study employed a standard approach for calculating adsorption isotherms, through certain modifications made considering previous research (Tan *et al*., 2021; Tan *et al*., 2023). Individual adsorbate solutions (Cu^{2+}/Pb^{2+}/Zn^{2+}) with concentrations ranging from 10 to 100 mg/L were prepared. The weight ratio between the adsorbent and the adsorbate solution was fixed at 1:50. All samples were prepared in triplicate. Each sample was placed in a 250 mL sealed conical flask in an incubator shaker for 24 h at 30 °C and at 100 rpm to achieve equilibrium. The samples were then centrifuged, and the concentrations of the solutions before and after adsorption were determined using inductively coupled plasma-optical emission spectrometry (ICP-OES). If necessary, a series of dilutions was performed to match the ICP-OES instrument's detection limit.

Adsorption Isotherms Analysis

For the analysis and interpretation of adsorption isotherms, two commonly used isotherm models, the Langmuir and Freundlich isotherms, were utilised to analyse the equilibrium data. The Langmuir adsorption model describes the surface as homogeneous with the assumption that maximum adsorption relates to a saturated monolayer of solute molecules occupied on the adsorbent's surface sites, with no lateral interaction between the adjacent adsorbed molecules, and the energy of adsorption is constant during the adsorption process (Benjelloun *et al.,* 2021). The Langmuir adsorption model is expressed as Equations 5 and 6.

$$q_e = \frac{q_m K_L C_e}{1+K_L C_e} \quad (5)$$

$$R_L = \frac{1}{1+(1+K_L C_e)} \quad (6)$$

Where q_e is the amount of adsorbate adsorbed (mg/g), C_e is the concentration of adsorbate at equilibrium (mg/L), q_m is the maximum adsorption capacity (mg/L), K_L is the Langmuir constant related to the energy of adsorption and R_L is a separation factor which indicates the nature of the adsorption process to be either unfavorable ($R_L > 1$), linear ($R_L = 1$), favorable ($0 < R_L < 1$), or irreversible ($R_L = 0$). The linearization of the Langmuir equation (Equation 7) can be used to determine the adsorption parameters.

$$\frac{C_e}{q_e} = \frac{1}{q_m K_L} + \frac{C_e}{q_m} \quad (7)$$

When C_e/q_e is plotted against C_e, a straight line with a slope of $1/q_m$ and an intercept of $\frac{1}{q_m K_L}$ is determined. The Freundlich adsorption isotherm model is widely applied for non-ideal adsorption on heterogeneous surfaces and describes the multilayer adsorption due to solute-solute interaction in the system. Freundlich isotherm also assumes the enthalpy of adsorption is independent of the amount adsorbed (Benjelloun *et al.,* 2021). The Freundlich model is expressed by Equation 8.

$$q_e = K_f C_e^{1/n} \quad (8)$$

Where, q_e is the amount of adsorbate adsorbed, C_e is the concentration of the adsorbate at equilibrium, K_f is the intercept at zero equilibrium concentration, and n is adsorption intensity. The linearization form of Equation 8 is given as Equation 9.

$$\log q_e = \log K_f + \frac{1}{n} \log C_e \quad (9)$$

The slope 1/n is a measure of adsorption intensity or surface heterogeneity, becoming more heterogeneous as its value gets closer to zero. A steep slope that is value of 1/n close to 1 reflects high sorption capacity at high equilibrium concentration, which decreases rapidly at lower equilibrium concentration. Whereas a flat slope with 1/n << 1 represents that the sorption capacity is slightly reduced at lower equilibrium concentration.

RESULTS AND DISCUSSION

Particle Size Distribution Analysis

Soil particle size distribution is crucial for understanding its effects on soil texture coarsening, degradation of soil structure and properties, as well as the movement of water and migration of solutes within the soil (Hailemariam *et al*., 2023). It also significantly affects the soil's adsorption capacity, as variations in particle composition determine the soil's ability to retain and bind ions, molecules, and pollutants (Yu *et al*., 2023). In the rubber plantation, orchard, and foothill areas, sand is the predominant component, ranging from 51.70 ± 0.05% to 42.11 ± 0.03%, classifying these soils as clayey sand (Table 2). The overall texture defined by the proportions of sand, clay, and silt can be interpreted through the chemical composition presented in Table 1. In contrast, hilltop soil is characterized as clay loam, with the highest clay content (39.87 ± 0.46%), followed by sand (37.81 ± 0.30%) and silt (22.32 ± 0.22%). This soil tends to experience minimal erosion due to stable vegetation cover, which promotes the gradual accumulation of finer particles like clay and silt, leading to the formation of clay loam. As soil materials move downslope, heavier sand particles tend to settle at the foothill, while lighter clay particles are more likely to be carried further by water or wind. This process results in a coarser soil texture at the base of the hill, forming clayey sand. Additionally, the orchard and rubber plantation soils undergo minimal mechanical disturbance due to infrequent tilling, which helps preserve their structure and maintain a relatively stable composition over time.

Table 2. Particle size distribution of soil samples.

Soil Texture	Rubber Plantation	Orchard	Hilltop	Foothill
Sand (%)	51.70±0.05	46.56±0.05	37.81±0.30	42.11±0.03
Clay (%)	30.24±0.04	27.32±0.02	39.87±0.46	36.75±0.01
Silt (%)	17.40±0.04	25.37±0.04	22.32±0.22	21.14±0.37

Surface Area Analysis

Table 3 shows the obtained results of the BET surface area, pore volume, and pore size of the studied adsorbents. All soil samples predominantly contain mesopores, with average pore sizes ranging from 12.61 to 24.07 nm. Hilltop soil exhibited a greater BET surface area (8.0020 m^2/g) and total pore volume (0.03343 cm^3/g) than foothill soil (7.0127 m^2/g, 0.02749 cm^3/g). This difference is likely attributed to the higher organic matter content in hilltop soil (Table 1), which reflects greater structural heterogeneity and influences both the original soil structure and its physicochemical properties. Rubber plantation soil possesses the lowest pore volume of 0.00070 cm^3/g, which might be influenced by the presence of low organic matter content. In contrast, orchard soil, despite having the largest pore size, maintains a higher pore volume than rubber plantation soil, likely a result of its richer organic matter and clay content. Soil specific surface area is closely related to particle size distribution, as a decrease in particle size leads to an increase in surface area. Clay particles, being smaller than sand, offer a significantly higher specific surface area. This expanded surface area enhances the soil's adsorption capacity by providing more surface for interactions with metals and other contaminants. A larger specific surface area also facilitates greater interaction between soil particles and ions or water molecules (Sepaskhah *et al.*, 2010). Therefore, soil with high specific surface areas has high adsorption capacity.

Table 3. Pore volume distribution and surface area of soil samples.

Adsorbent	BET surface area (m^2/g)	Total pore volume (cm^3/g)	Pore size (nm)
Orchard	4.3006	0.01462	24.07
Rubber Plantation	3.3249	0.00070	18.78
Hilltop	8.0220	0.03343	14.23
Foothill	7.0127	0.02749	12.61

The nitrogen (N_2) adsorption and desorption isotherm curves along with pore size distribution data, were analyzed to compare the adsorption behavior across four soil types. As illustrated in Figure 1, the isotherms correspond to a typical Type II profile, indicative of unrestricted monolayer to multilayer adsorption. The adsorption/desorption isotherm curves exhibited a very low adsorption and desorption in low relative pressure region; and a steep monolayer adsorption are found above the partial pressure (P/P_0) around 0.5– 0.9 suggesting the presence of mesopores in the soil samples. The desorption isotherm curves for all soil samples exhibit the characteristic H3 hysteresis loop (capillary condensation occurs) given by non-rigid aggregates of plate-like particles which further indicate the existence of mesopores in the studied adsorbents.

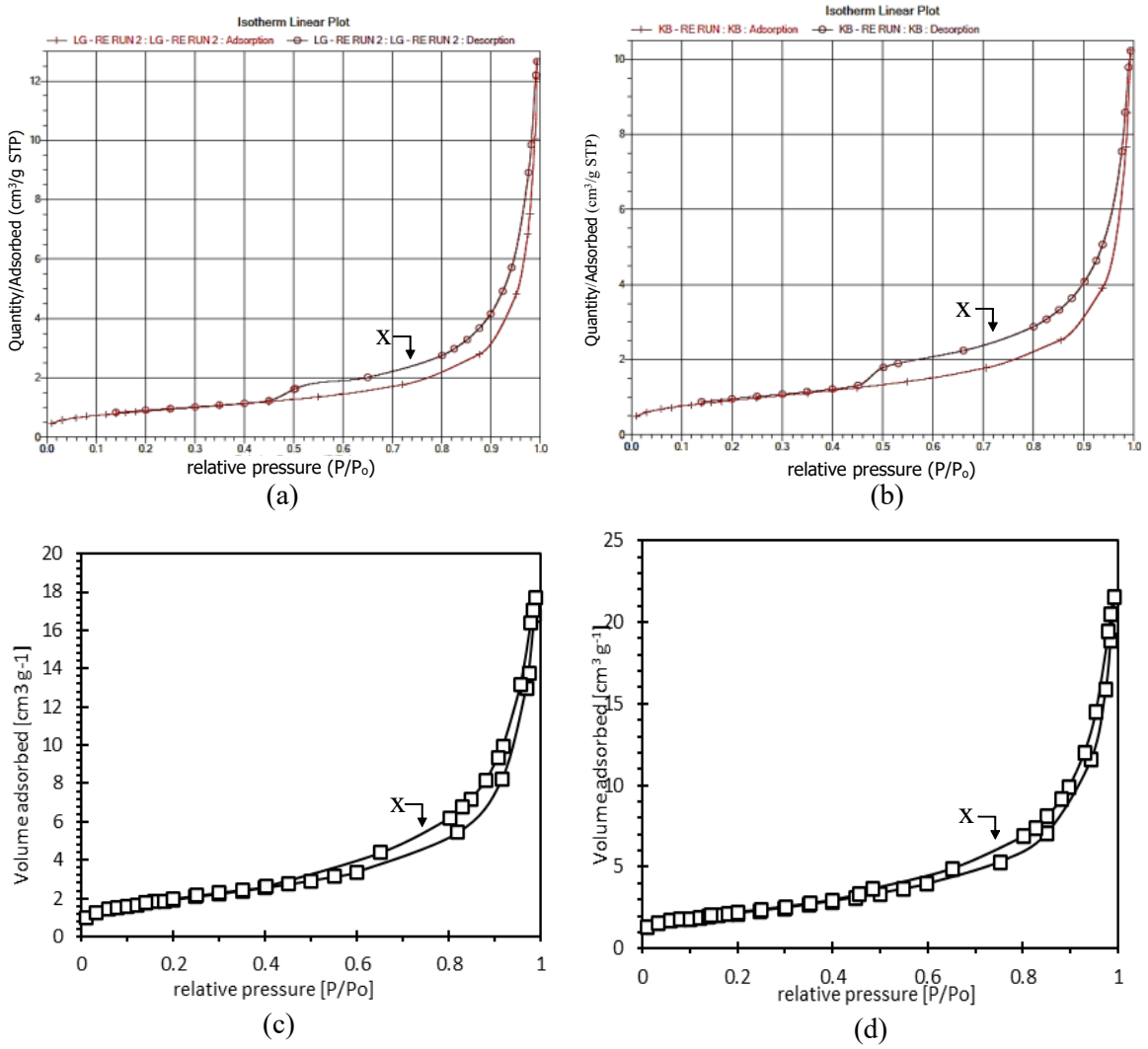

Note: x – desorption

Figure 1. N_2 adsorption/desorption isotherms of (a) orchard soil, (b) rubber plantation soil, (c) hilltop soil, and (d) foothill soil.

Cation Exchangeable Capacity (CEC) Analysis

It is found that the clay loam soil (hilltop) exhibited the highest CEC value of 35.060 ± 0.004 $cmol_c$ /kg compared to clayey sand soils (24.170 ± 0.002, 20.285 ± 0.001, and 12.371 ± 0.002 $cmol_c$/kg) from other sampling sites (Table 4). Clayey sand soils exhibit lower cation exchange capacity (CEC) due to their larger particle size (reflected in the higher sand content shown in Table 2) and reduced negative surface charge. This larger size produces a smaller surface-to-volume ratio, reducing the availability of negative sites to attract cations, including heavy metal ions in this context (Abegunde *et al.*, 2020). Theoretically, clayey sand soils exhibit lower adsorption capacity due to their coarse texture leads to larger pore spaces. As soil particle size increases, adsorption tends to decrease; conversely, finer particles exhibit greater adsorption capacity. Clay particles possess a high surface area and elevated CEC, enabling them to retain more positively charged ions such as nutrients and metals. Therefore, soils with higher clay content typically demonstrate enhanced adsorption capacity for these ions (Chen *et al*., 2023). The adsorption capacity of soil is expected to rise with increasing clay composition.

Table 4: CEC value of soil samples.

Soil Samples	CEC ($cmol_c$ /kg)
Orchard	20.285 ± 0.001
Rubber Plantation	12.371 ± 0.002
Hilltop	35.060 ± 0.004
Foothill	24.170 ± 0.002

Organic matter plays a crucial role in enhancing the soil's cation exchange capacity (CEC). It contains functional groups such as oxidized carboxylate and phenolate, which generate negative charges, particularly under higher pH conditions, making organic matter a significant contributor to CEC. Despite having similar chemical compositions and particle size distributions, orchard soil demonstrates a notably higher CEC value (20.285 ± 0.001 $cmol_c$/kg) than rubber estate soil, largely due to its substantially greater organic matter content (4.38 ± 0.03%) compared to that of rubber estate soil (1.99 ± 0.01%) (Table 1). In the case of hilltop versus foothill soils, elevation differences lead to distinct temperature regimes. Higher elevations experience cooler temperatures, which promotes the accumulation of organic matter in hilltop soils (Kumar *et al.,* 2019). These lower temperatures suppress microbial and enzymatic activity, thereby slowing the decomposition of organic material. Consequently, the reduced biological breakdown at high altitudes is a key factor driving the elevated organic matter content in hilltop soils.

Adsorption Isotherms

The amounts of adsorbed heavy metals, q_e, and the equilibrium concentrations, C_{eq} are plotted and shown in Figure 2. The amount of adsorption toward heavy metals increases with rising equilibrium concentrations. The adsorption isotherm curve clearly showed that the adsorption rate of Cu^{2+}, $Pb^{2+,}$ or Zn^{2+} in the soil sample was rapid at lower concentrations and gradually decreased to reach a maximum value. This behavior explains that in lower concentrations, heavy metal ions exhibit high mobility and therefore, enhance their interaction with soil samples (adsorbents). However, as the concentrations increase, the binding centers of the soil samples become saturated because the amount of heavy metal ions exceeds the number of available adsorption sites, preventing further adsorption (Sangiumsak & Punrattanasin, 2014). Besides, the increase in heavy metal ion concentration has affected the amount of heavy metal ions adsorbed due to the increased driving force of these ions towards the active sites of soil samples. Therefore, the adsorption rate is getting lower as the concentration of heavy metal ions increases.

The Langmuir and Freundlich isotherms were adopted to describe the adsorption isotherm. Table 5 shows the parameters of both Langmuir and Freundlich isotherms. Both adsorption isotherms exhibited R^2 values predominantly above 0.93, indicating that both models can accurately describe the isotherm behavior. Analysis revealed that the Freundlich isotherm performs equally well as the

Langmuir isotherm in modeling adsorption behavior. The consistency of the Langmuir isotherm implies that adsorption occurred in the form of a monolayer of metal particles on the soil surface.

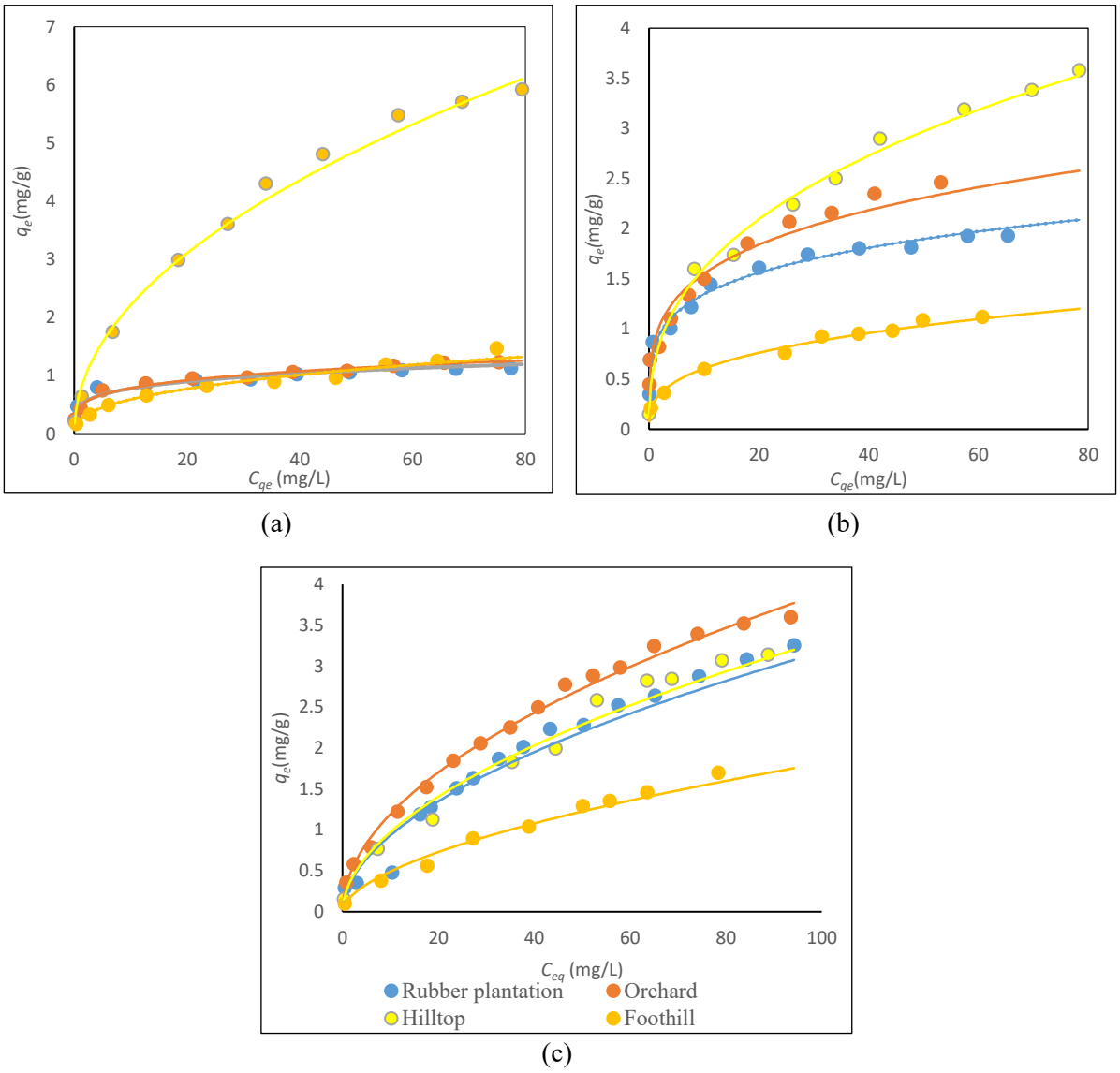

Figure 2. Adsorption isotherm of (a) Cu^{2+}, (b) $Pb^{2+,}$ and (c) Zn^{2+}.

The clay loam soil from the hilltop exhibited the highest adsorption capacity, with the metal ion affinity following the order of $Cu^{2+} > Pb^{2+} > Zn^{2+}$. In contrast, clayey sand soils from orchards, rubber plantations, and the foothill region exhibited a preference for Zn^{2+} over Pb^{2+} and Cu^{2+}, indicating a distinct adsorption pattern despite sharing a similar soil classification. This variation implies that metal adsorption behavior in clayey sand soils is influenced not only by soil type but also by other factors such as mineral composition, organic matter levels, and land management practices.

The hilltop soil, classified as clay loam and exhibiting a higher proportion of clay particles (Table 2), offers more binding sites for heavy metal ions, resulting in a greater overall adsorption capacity compared to clayey sand soil. The particle size of clay is smaller than sand particles and produces a greater specific surface area relative to their size (Table 3). High clay content also provides higher cation exchange capacity (CEC). Moreover, the presence of organic matter further supports adsorption by forming stable organo-metallic complexes. In contrast, clayey sand soils (orchard, rubber plantation, and foothill soils) display distinct mineralogical compositions, particularly in the types of clay minerals and iron/ aluminium oxides present (Table 1). Differences in land use and topography also

result in variations in soil organic matter content and pH, even within similar textural classes. These factors influence the availability of sites for adsorption and the sequence in which adsorption occurs, thereby affecting the adsorption capacity of the soil, which reflects its ability to retain and immobilize substances such as heavy metals.

Table 5: Parameters of Langmuir and Freundlich.

Soil	Metal	Langmuir				Freundlich		
		q_m	K_L	R_L	R^2	n	K_f	R^2
Orchard	Cu^{2+}	1.261	0.233	0.046	0.9881	4.422	0.720	0.9805
	Pb^{2+}	2.560	0.381	0.028	0.9959	2.978	0.891	0.9643
	Zn^{2+}	3.743	0.033	0.251	0.9379	1.751	0.535	0.9957
Rubber Plantation	Cu^{2+}	1.137	0.583	0.022	0.9907	6.230	0.782	0.9669
	Pb^{2+}	2.151	0.770	0.016	0.9989	3.481	0.908	0.9349
	Zn^{2+}	3.350	0.053	0.192	0.9455	1.991	0.608	0.9453
Hilltop	Cu^{2+}	6.139	0.003	0.666	0.9957	1.021	0.033	0.9813
	Pb^{2+}	3.792	0.035	0.159	0.9387	3.831	0.874	0.9361
	Zn^{2+}	3.451	0.014	0.328	0.9326	1.489	0.099	0.9303
Foothill	Cu^{2+}	1.403	0.469	0.030	0.9833	1.021	0.033	0.9413
	Pb^{2+}	1.134	0.160	0.082	0.9352	2.115	0.196	0.9336
	Zn^{2+}	1.859	0.006	0.824	0.9408	1.145	0.080	0.9409

CONCLUSION

The adsorption characteristics of the studied soils were effectively described by both Freundlich and Langmuir isotherm models. Clay loam soil (hilltop) exhibited higher adsorption capacity, whereas clayey sand soils (orchard, rubber plantation, and foothill) demonstrated the lowest. All soils showed measurable sorptive potential, with distinct metal ion affinities governed by their physicochemical properties. Adsorption capacity was primarily influenced by factors such as mineralogical composition, particle size distribution, organic matter content, cation exchange capacity, pH, and specific surface area. A comprehensive understanding of these soil attributes is essential for accurately predicting adsorption behavior and conducting site-specific evaluations of heavy metal retention potential.

ACKNOWLEDGEMENT

The authors gratefully acknowledge Universiti Malaysia Sabah (UMS) for the funding with grant number SBK0486-2021.

REFERENCES

Abegunde, S.M., Idowu, K.S., Adejuwon, O.M. & Tinuade, A., 2020. A review on the influence of chemical modification on the performance of adsorbents. *Resources, Environment and Sustainability,* 1:100001.

Ali, J.K., Ghaleb, H., Arangadi, A.F., Le, T.P.P., Moraetis, D., Pavlopoulos, K. & Alhseinat, E. 2023. Comprehensive assessment of the capacity of sand and sandstone from aquifer vadose zone for the removal of heavy metals and dissolved organics. *Environmental Technology & Innovation*, 29: 102993.

ASTM D7928-21E1: Standard Test Method for Particle-Size Distribution (Gradation) of Fine-Grained Soils Using the Sedimentation (Hydrometer) Analysis.

ASTM E1727-20: Standard Practice for Field Collection of Soil Samples for Subsequent Lead Determination

Ayangbenro, A.S. & Babalola, O.O., 2017. A new strategy for heavy metal polluted environments: a review of microbial biosorbents. *International Journal of Environmental Research and Public Health,* 14: 94; doi:10.3390/ijerph14010094.

Bai, B., Bai, F. & Hou, J. 2024. The migration process and temperature effect of aqueous solutions contaminated by heavy metal ions in unsaturated silty soils. *Heliyon*, 10(9): e30458.

Benjelloun, M., Miyah, Y., Evrendilek, G. A., Zerrouq, F. & Lairini, S. 2021. Recent advances in adsorption kinetic models: Their application to dye types. *Arabian Journal of Chemistry*, 14(4): 103031.

Chen, J., Yuan, J., Tong, H., Fang, Y. & Gu, R. 2023. Mechanism study on the soil mechanical behavior of the mixed soil based on energy multi-scale method. *Frontiers in Materials*, 10.

Chenu, C., Rumpel, C., Védère, C. & Barré, P. 2024. Methods for studying soil organic matter: nature, dynamics, spatial accessibility, and interactions with minerals. *In Elsevier eBooks* (pp. 369–406).

Hailemariam, M.B., Woldu, Z., Asfaw, Z. & Lulekal, E. 2023. Impact of elevation change on the physicochemical properties of forest soil in South Omo Zone, southern Ethiopia. *Applied and Environmental Soil Science*, 1–17.

ISO 9277:2010(E). Determination of the specific surface area of solids by gas adsorption - BET method.

Kumar, S., Suyal, D.C., Yadav, A., Shouche, Y. & Goel, R. 2019. Microbial diversity and soil physiochemical characteristics of higher altitude. *Plos One*, 14(3).

Musilova, J., Arvay, J., Vollmannova, A., Toth, T. & Tomas, J., 2016. Environmental contamination by heavy metals in region with previous mining activity. *Bulletin of Environmental Contamination and Toxicology*, 97: 569-575

Naveedullah, Hashmi, M.Z., Yu, C.N., Shen, H., Duan, D.C., Shen, C.F., Lou, L.P. & Chen, Y.X., 2013. Risk assessment of heavy metals pollution in agricultural soils of siling reservoir watershed in Zhejiang Province, China. Hindawi Publishing Corporation. *BioMed Research International,* Volume 2013, Article ID: 590306, 10 pages http://dx.doi.org/10.1155/2013/590306

Olaniran, A.O., Balgobind, A. & Pillay, B. 2013. Bioavailability of heavy metals in soil: impact on microbial biodegradation of organic compounds and possible improvement strategies. *International Journal of Molecular Sciences*, 14: 10197-10228

Sangiumsak, N. & Punrattanasin, P. 2014. Adsorption behavior of heavy metals on various soils. *Polish Journal of Environmental Studies.,* 23(3): 853-865

Sepaskhah, A.R., Tabarzad, A. & Fooladman, H.R., 2010. Physical and empirical models for estimation of specific surface area of soils. *Archives of Agronomy and Soil Science*, 56: 325–335.

SW-846 Method 9080: 1986. Cation-Exchange Capacity of Soils (Ammonium Acetate), Part of Test Methods for Evaluating Solid Waste, Physical/Chemical Methods.

Tan, W.H., Surugau, N., Bahrun, M.H.V. & Bono, A. 2021. Heavy metal Cu(II) and Pb(II) retention on clay soil. In *Proceedings of the Seminar on Science and and Technology 2021*, pp. 42-44, Sabah, Malaysia.

Tan, W.H., Surugau, N., Bono, A., Bahrun, M.H.V., Idris, R., Ali, S.A.M., Tair, R. & Rahim, S.A. 2023. Effect of soil composition in copper (II), lead (II), and zinc (II) ion adsorption capacity. *Science, Engineering and Health Studies*, 17: 23020001.

Yu, H., Li, C., Yan, J., Ma, Y., Zhou, X., Yu, W., Kan, H., Meng, Q., Xie, R. & Dong, P. 2023. A review on adsorption characteristics and influencing mechanism of heavy metals in farmland soil. RSC Advances, 13(6): 3505 – 3519.